RSC Advances

ROYAL SOCIETY OF CHEMISTRY

www.rsc.org/advances

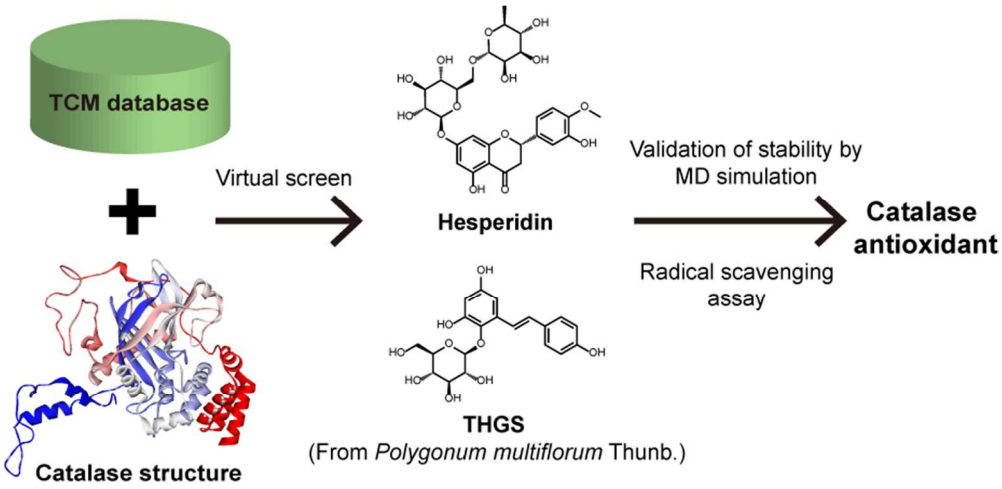

78x38mm (300 x 300 DPI)

Insight into two antioxidants binding to the catalase NADPH binding site from traditional Chinese medicines

Hung-Jin Huang [1], Hsin-Yi Chen [2], Yuan-Shiun Chang [1*], Calvin Yu-Chian Chen [2, 3, 4 *]

[1] *Department of Chinese Pharmaceutical Sciences and Chinese Medicine Resources, College of Pharmacy, China Medical University, Taichung 40402, Taiwan.*

[2] *Department of Biomedical Informatics, Asia University, Taichung, 41354, Taiwan.*

[3] *Human Genetic Center, Department of Medical Research, China Medical University Hospital, 40402 Taichung, Taiwan*

[4] *Research Center for Chinese Medicine & Acupuncture, China Medical University, Taichung 40402, Taiwan.*

*Correspondence should be addressed to Yuan-Shiun Chang; yschang@mail.cmu.edu.tw and Calvin Yu-Chian Chen; ycc929@MIT.edu

Abstract

Catalase is an important enzyme performs decomposition of two molecular of hydrogen peroxide to water molecules and oxygen in aerobic organism. Deficiency or inactive catalase are implicated cell damage and lead to inflammation, aging and cancer. In order to develop novel nature product that prevent inactive catalase generation, the world largest traditional Chinese medicine (TCM) database (http://tcm.cmu.edu.tw/) were employed to this study, which combined with high-throughput virtual screening and molecular dynamics (MD) simulation to investigate potent nature compounds for keeping catalase active. We found the two nature product, Hesperidin and 2,3,5,4'-tetrahydroxystilbene-2-O-β-D-glucoside (THSG), the found ligands perform high binding affinity with catalase. The results of MD simulation show that THSG is the most stable in trajectory analysis over all simulation times. Besides, THSG can affect the catalase structure more compact during the process of MD simulation. In addition, the radical scavenging assay showing that THSG has more potential antioxidant activity than Hesperidin. Therefore, we regard the nature TCM compound, THSG, could be used to develop potential drugs that might have similar effect to keep catalase active and prevent the inactive form generation by hydrogen peroxide.

Key words: radical scavenging, Traditional Chinese Medicine (TCM), antioxidant,

catalase, docking, drug design, molecular dynamics (MD) simulation

1. Introduction

Catalase is a heme-enzyme and ubiquitous present in living organisms, the function of catalase is to destroys hydrogen peroxide (H_2O_2) to two molecules of water and one molecule of oxygen [1, 2], which is an important enzyme to against oxidative damage in cell and tissues. The reaction of catalytic in decomposition of hydrogen peroxide to water and oxygen as follow [3, 4]:

$$2\ H_2O_2 \rightarrow 2\ H_2O + O_2$$

Reactive oxygen species (ROS) were produced from aerobic organism, that including superoxide anion, hydroxyl radical, and hydrogen peroxide. In normal metabolism, ROS are scavenged by antioxidant enzyme such as superoxide dismutase [5-7], glutathione peroxidase [8-10] and catalase [11-14]. Hydrogen peroxides are linked to cellular damage. In some cases of catalase deficiency [15-17], the increased levels of hydrogen peroxide and free radicals concentrations contribute to oxidative damage in DNA, proteins, and cells.

When catalase expose to H_2O_2, nicotinamide adenine dinucleotide phosphate (NADPH) could tightly bind to catalase and prevent the inactivation of catalase by H_2O_2 [18]. During the process of disposing H_2O_2, NADPH binds to mammalian catalase and serves to protect the formation of the enzyme to an inactive form (compound II)

[19]. In addition, the processes of removing H_2O_2 through glutathione reductase and glutathione peroxidase are also require NADPH during oxidative stress condition [20], but some studies denote that the role of NADPH in keeping catalase active is more important than glutathione reductase and peroxidase [21, 22]. The purpose of this study is to discover more potent TCM compounds to prevent inactive catalase accumulation.

For developing new drugs, computer-aided drug design (CADD) has been widely used in many studies [23-26] and combined with risk factors study [27], which could accelerates the development of leading drugs [28, 29]. Traditional Chinese medicine (TCM) has been used for thousand years in many Asian countries, and some experiments using TCM to discover novel nature compounds to investigate new treatment [30, 31]. In order to identify more potential compounds for keeping catalase active, we used TCM Database@Taiwan (http://tcm.cmu.edu.tw/) [32] to investigate potential small molecules through database virtual screening. In further analysis, molecular dynamics (MD) simulations were employed to simulate the protein-ligand complexes in dynamics condition to observe the variation of protein structure and stability of all systems. The selected TCM compounds were further examined the radical scavenging to determine the anti-oxidant ability, and the radical scavenging experiments were using DPPH and Trolox equivalent methods. The results from database virtual screen and radical scavenging assay will help to facilitate in

discovery of more potential nature compound from TCM database for inactive catalase generation.

2. Materials and Methods

2.1 Protein preparation and validation

Protein structure of human catalase was downloaded from Protein Data Bank (PDB ID: 1DGF) [33], all residues are protonated at pH 7.4 and corrected missing atoms and loops by *Prepare Protein module* under Accelrys Discovery Studio 2.5.5.9350 (DS 2.5) [34]. In protein structure validation, the disorder prediction tool, PONDR-FIT [35], was employed to identify the ordered region on the catalase sequence, and sequence (Entry: P04040) was obtained from Uniprot database.

2.2 Docking study

We according to ADMET of pharmacology [36] and Lipinski's Rule of Five [37, 38] to evaluate drug-likeness of 61,000 TCM compounds, all TCM compound with drug-likeness being used for docking analysis of catalase structure under LigandFit module in DS 2.5. The Monte-Carlo techniques generated different ligand poses for protein-ligand interaction analysis. The CHARMm force field [39] described all ligand conformation for energy minimization. The minimization performed 1000 step and following by Conjugate Gradient. Docking results were based on -PLP1, -PLP2,

-PMF and Dock Score to select top candidates. All of the docking poses were visualized by DS 2.5 [34] and LigPlot plus software [40]

2.3 Molecular Dynamics (MD) Simulation

MD simulation of protein-ligand complexes were performed by GROMACS 4.5.5 [41] with charmm27 force field. The cutoff distance of box definition was defined as 1.2 nm, and the solvent model used TIP3P for water modeling. For system neutralization, Na and Cl ions were random replaced water molecules, the concentration of NaCl model was set to 0.145 M. The linear constraint solver (LINCS) algorithm constrained all bonds of simulation systems to fix all bond lengths. We employed SwissParam web server [42] to generate the topology files and parameters of top candidates and control form docking results. The coulomb type of electrostatics was calculated by Particle mesh Ewald (PME) method, 1.4 nm cut-off distance was used for van der Waals (VDW) interactions. The first step of MD simulation performed 5,000 cycle steps of Steepest Descent algorithm for energy minimization. In the second step, equilibration performed 1ns under constant temperature dynamics (NVT type) conditions for position restraints. The final step was performed 5000 ps of production run under constant pressure and temperature dynamics (NPT type). The temperature was set to 310K over all simulation times. MD frames data were

collected over production run every 20 ps.

2.4 MD analysis

Root mean square deviation (RMSD) and radius of gyration (Rg) were analyzed by the command g_rms and g_gyrate under GROMACS 4.5.5 software, respectively. The total energy of simulation systems were evaluated by the g_energy program. The Root mean squared fluctuation (RMSF) of protein residues was calculated by g_rmsf. The g_dist program was used to measure the distance between protein and ligand for movement analysis. Mean square displacement (MSD) was performed by g_msd module to observe the migration of docked ligand during the simulation time. In order to select the represented structure from all MD frames, g_cluster program was carried out for cluster analysis. For ligand path prediction, Caver 3.0 software [43] was employed to predicted tunnels of docked ligand in Catalase.

2.5 DPPH radical-scavenging activity

The radical-scavenging assay [44, 45] was measured using the DPPH (1,1-diphenyl-2-picrylhydrazyl radical) for detecting the anti-oxidant activity of TCM compounds. The DPPH was dissolved in methanol to give concentration of 202.9 μM (80 μg/mL). The initial concentrations of Hesperidin and THGS (test compounds in this study) were 393.08 μM (240 μg/mL) and 364.19 μM (148 μg/mL), respectively.

We further used methanol to give dilutions (Hesperidin: 195.0 μM, 92.5 μM; THGS: 182.05 μM, 91.025 μM) of the test compounds for DPPH radical-scavenging assay. We used BHT (2,6-bis(1,1-dimethylethyl)-4-methylphenol) as positive control and dissolved in methanol solution for comparing antioxidant activity with test compounds. BHT was diluted to suitable concentrations of 3358 μM (740 μg/mL), 1679 μM (370 μg/mL), and 839.5μM (185 μg/mL) to find the effective concentration (EC_{50}). The inhibition percentage (%) of DPPH radical scavenging activity was calculated using the equation (1)

$$\text{Inhibition (\%)} = (Ao - As)/Ao \times 100 \quad (1)$$

Where *Ao* is the absorbance of the control and *As* is the absorbance of the sample at 517 nm. The 50% effect of equivalent concentration (EC_{50}) was currently used in the interpretation of DPPH radical scavenging data. The test compounds (hesperidin and THGS) and BHT were mixture with DPPH and reacted for 20 minutes in the dark condition at room temperature, and then measured under absorbance of 517 nm by ELISA (enzyme-linked immunosorbent assay). Above reaction of each sample was repeated three times to obtain mean ± SD (n=3).

2.6 Trolox equivalent antioxidant capacity (TEAC) assay

We utilized 2,2'-azinobis-3-ethylbenzotiazoline-6-sulphonic acid (ABTS) to

evaluate the anti-oxidant activity of TCM compounds. The TEAC assay was developed by Miller et al. for measuring the antioxidant capacity [46]. The $ABTS^+$ was obtained from the mixture solution that contains 7mM of ABTS and 2.45mM of potassium persulfate for 16 hour reaction. $ABTS^+$ was used to mixture with different concentrations of Trolox. The contain of $ABTS^+$ radical was measured at 734 nm after 1 minute reaction time for giving Trolox equivalents, the calibration curve was constructed from concentrations of Trolox with 0, 10, 20, 50, 100, 250, 500, 1000 μM. The absorbance of TCM compounds (hesperidin and THGS) and positive control (BHT) were based on calibration curve to calculate the equivalent values of Trolox. Above reaction of each sample was repeated three times to obtain mean ± SD (n=3).

3. Results and Discussion

3.1 Docking analysis

To select high affinity compound for catalase interaction, we according to different scoring functions such as -PMF, Dock Score, -PLP1, and -PLP2 for analyzing affinity between catalase and each ligand (Table 1), candidates from docking results were ranked by -PMF score. The high values of -PMF and Dock Score indicate more binding affinity between protein and ligand. The -PLP1 and -PLP2 score express the ability of small molecule to generate H-bond for protein

interaction. NADPH was regarded as control to comparing with docking compounds. In binding affinity analysis, we found that the DockScore of Hesperidin and 2,3,5,4'-tetrahydroxystilbene-2-O-β-D-glucoside (THSG) are higher than Cordyceamides A and Grandisin. In addition, all of scoring functions of Hesperidin and THSG are higher than NADPH. Hence, we selected these two TCM compounds for binding poses study. About resources of these two TCM compounds, Hesperidin could be extracted from unripe fruit of *Citrus aurantium*; [47] and THGS is available in *Polygonum multiflorum* [48]. The chemical scaffold of selected ligands and NADPH are shown in Figure 1. For pi interactions analysis on 2D diagram of docking pose, Hesperidin displays one pi-interaction on Arg203 (Figure 2a), THSG has two pi-interactions on His305 and Arg203 (Figure 2b), NADPH reveals one pi-interaction on His305 (Figure 2c). Figure 2 also provided information about H-bonds generation between ligand and residue, the 2D diagram showing that Hesperidin forms one H-bond on Ser201, THSG forms two H-bonds on Trp303 and Arg203, NADPH displayed two H-bonds Arg203 and Lys237. To visualize hydrophobic interaction between protein and ligand, we employed LigPlot plus program to descripted protein-ligand interaction diagrams for showing residues with hydrophobic force, the most common residues with hydrophobic are Phe198, Arg203, Tyr215, Val302, Phe446, and Val450 (Figure 3). Here, we concluded key residues form Figure 2 and

Figure 3, the key residues are Pro151, His194, Phe198, Arg203, Asn213, Tyr215, Lys237, Val302, Pro304, His305, Lys306, Gln442, Phe446, and Val450. To understand these key residues are located in folded structure of catalase, we utilized PONDR-FIT to obtain Disorder Disposition values of each residues, the prediction result was shown in Figure 4. The results of disorder prediction reveal that the key binding residues (blue line) are belong to ordered structure, the plot shows disorder dispositions value of each key residue are below 0.5. The disorder folding region will causes drug side-effect through ligand binding [49], the binding region should be ordered folding structure [50, 51] to design a drug which could stable bind to a protein. Therefore the binding site of catalase has no effect on docking process of ligands. In next study, we performed MD simulation to observer the complexes with selected compounds in dynamics condition.

3.2 Trajectory analysis

To assess the stability of the dynamic frames of catalase with docked ligands, we calculated root mean-square deviation (RMSD) values of all frames by the first conformation, the RMSD plots of each protein and ligand were displayed in Figure 5. For Protein RMSD, complex of Hesperidin tends to stability with an average of 0.45

nm after 2ns. The protein of THGS complex reveals stable fluctuation after 4.5 ns. For NADPH complex, the Protein RMSD shows stability after 1ns. All of Protein RMSD values illustrated protein structures turned to stable within a simulation time of 5 ns. For Ligand RMSD, THSG has the lowest fluctuation over 5 ns. Hesperidin exhibits two peaks before 1ns and consequently turned to stability until last simulation time. NADPH displays flexible in the period from 0ns to 2ns, and then stabilize the fluctuation with an average of 0.45 until the end of simulation time. The data of Ligand RMSD showing that the ligand conformation of NADPH is significant difference with initial binding pose. For gyration analysis, all conformations of each protein complex performs compact structure gradually during simulation time of 5ns (Figure 6a), we also observed that the gyrate values of complexes with TCM candidates were under 2.5 nm earlier than NADPH. It is worth to note that the complex of THSG first to generate compact conformation at 2ns, which suggest THSG has more ability to stabilize the structure of catalase than Hesperidin and NADPH. In ligand migration analysis, the Hesperidin and THSG exhibit low mean square deviation (MSD) values during simulation time of 5ns (Figure 6b), but the MSD values of NADPH reveals increased from 0 ns to 4.5 ns, indicated that NADPH migrated from initial position progressively, and this result is consistent with Ligand RMSD analysis.

3.3 Total energy calculation and flexibility analysis

In energy analysis, we calculated the total energy of all simulation systems over all simulation times, there are no substantial fluctuation was observed from energy calculation (Figure 7), all of total energy values are within 10,000 KJ/mol, which showing the systems performed stable condition during MD simulation. To analyze the fluctuation of each residue, we calculate root mean square fluctuation (RMSF) to observe the flexibility of key residues. From RMSF analysis, the large fluctuated residues are exhibit in the region from residue index 375 to 425 (Figure 8), indicating that key residues Gln442, Phe446, and Val450 are not suitable for ligand binding. To identify the stable period of simulation time, we clustered all dynamic frames to identify the suitable conformation of catalase complex. For cluster analysis, we found the largest groups were observed in the period from 2ns to 5ns (Figure 9), therefore we considering the period of simulation time to be reliable period of time in further studies.

3.4 Distance analysis

We measured the distance of center of mass between protein and ligand during a simulation time of 5ns. Interestingly, the distance between NADPH and catalase are

longer than TCM candidates, THSG has the shortest distance during all simulation times, and the result is also consistent with Ligand RMSD analysis and Gyration analysis. In H-bond distance analysis, we calculated the distance between acceptor and donor atoms for observing stable H-bonds. Comparing with the key residues from docking study, Arg203, Tyr215, Lys237, His305, and Lys306 are still formed H-bond (Figure 11), the H-bond distance of these residues with an average of 0.3 nm.

3.5 Stability of MD conformation

To analyze the stability of all MD conformation, the DSSP program were used to visualize the secondary structure over all simulation times, the key residues including Arg203, Tyr215, Lys237, His305, and Lys306 are locate in the region from residue index 200 to 350 (Figure 12), which reveal that each type of secondary structure are remain stable during 5ns, and indicate the structure are not variable through protein-ligand interaction. We further calculated the smallest distance between each pair residues for catalase, the matrices of the smallest distance are similar to each other (Figure 13), which showing that all structure of protein complexes are stable over all simulation times. For analyzing the motion of protein structure, principal component analysis (PCA) was used to measure all MD frames, the eigenvalues of

first two eigenvectors (PC1 and PC2) were calculated in Figure 14, the data showing that Hesperidin and THSG have short range of eigenvalues than NADPH in PC1 and PC2, we further comparing PC1 and PC2 in phase space (Figure 15), the points of NADPH are distributed and cannot cluster into groups, which indicated that the protein motion of NADPH are broad than Hesperidin and THSG. In ligand tunnel prediction, we found that NADPH generated more ligand channels than Hesperidin and THSG (Figure 15), which suggest that NADPH has high opportunity to except from docking position, the result illustrates Hesperidin and THSG have more resident time in catalase binding site. The data of ligand tunnel prediction also shows that THSG has the smallest size of predicted channels, combining with all results of MD analyses; THSG could be regarded as potential lead compound to bind to catalase for prevent catalase inactive.

3.6 Antioxidant activity of Hesperidin and THSG

The MD simulation showing the THSG is more potential for interacting with catalase than Hesperidin, we further used DPPH radical scavenging method and TEAC assay to assess the ability of antioxidant for Hesperidin and THSG. The DPPH analysis reveals that Hesperidin has no activity of EC_{50} value with concentration of

240μg/mL (Table 2), but THGS displayed 105.80 of EC_{50} and higher than BHT. For TEAC assay, we used calibration curve to evaluate the antioxidant activity of test compounds (Figure 17). The result of TEAC shows that the THGS has most activity value of antioxidant than Hesperidin and BHT (Table 3), which illustrate that THGS performed more potential antioxidant activity than Hesperidin.

4. Conclusion

In summary, we based on -PLP1, -PLP2, -PMF, and Dock Score for filtering candidates, Hesperidin was predicted to have the highest score in docking result, but MD analyses showing that THSG reveals more potential to affect catalase conformation than Hesperidin. The result of disorder prediction showed that the key residues from docking pose are ordered folding structure, which indicated the docking site has no side-effect by ligand bound. Form trajectory analyses, stability of THSG-catalase complex suggest that THSG promote catalase compact and stabilize among all simulation times, we also observed the variation of protein conformation by RMSF calculation, DSSP analysis, PCA analysis, and matrices of small distance calculation, THSG-catalase complex reveals no substantial fluctuation after simulation time of 5ns. We also analyze the results of Ligand RMSD and MSD, these data illustrate that the binding conformation of THSG has no significant change. In

addition, the protein-ligand distance is also consistent with Ligand RMSD and MSD analysis, this comparison provides evidences to explain that THSG has potential to affect catalase. H-bond distance reveals key residues: Arg203, Tyr215, Lys237, His305, and Lys306 still formed H-bond with TCM candidates and NADPH, and these residues could be regarded as important amino acids for catalase binding. The antioxidant activity assays also confirm that THGS has highest radical scavenging ability than Hesperidin. The role of NADPH bind to catalase is to keep catalase active, our found ligands not only have anti-oxidant ability but also had good binding ability to interact with catalase. The two TCM compounds, Hesperidin and THGS, might have similar effect with NADPH to affect catalase, which may be potential anti-oxidant drug in further research, and help for keeping catalase active during decomposition of hydrogen peroxide.

Acknowledgements

The research was supported by Grants from the National Science Council of Taiwan (NSC102-2325-B039-001 and NSC102-2221-E-468-027-), Asia University (ASIA100-CMU-2, ASIA101-CMU-2, and 102-Asia-07), and China Medical University Hospital (DMR-103-058, DMR-103-001, and DMR-103-096).This study is also supported in part by Taiwan Department of Health Clinical Trial and Research

Center of Excellence (DOH102-TD-B-111-004), Taiwan Department of Health Cancer Research Center of Excellence (MOHW103-TD-B-111-03), and CMU under the Aim for Top University Plan of the Ministry of Education, Taiwan.

Conflict of Interests

The author(s) confirm that this article content has no conflicts of interest.

References

1. I. von Ossowski, G. Hausner and P. C. Loewen, *J Mol Evol*, 1993, 37, 71-76.
2. C. M. Griswold, A. L. Matthews, K. E. Bewley and J. W. Mahaffey, *Genetics*, 1993, 134, 781-788.
3. S. Mishra and J. Imlay, *Arch Biochem Biophys*, 2012, 525, 145-160.
4. T. P. Ko, M. K. Safo, F. N. Musayev, M. L. Di Salvo, C. Wang, S. H. Wu and D. J. Abraham, *Acta Crystallogr D Biol Crystallogr*, 2000, 56, 241-245.
5. H. P. Misra and I. Fridovich, *J Biol Chem*, 1972, 247, 3170-3175.
6. R. J. Branco, P. A. Fernandes and M. J. Ramos, *J Phys Chem B*, 2006, 110, 16754-16762.
7. A. L. Brioukhanov and A. I. Netrusov, *Biochemistry (Mosc)*, 2004, 69, 949-962.
8. C. Victorrajmohan, K. Pradeep and S. Karthikeyan, *Drugs R D*, 2005, 6, 395-400.
9. V. M. Tenorio-Velazquez, D. Barrera, M. Franco, E. Tapia, R. Hernandez-Pando, O. N. Medina-Campos and J. Pedraza-Chaverri, *BMC Nephrol*, 2005, 6, 12.
10. V. Ramos, A. Valenzuela, E. Villanueva and M. T. Miranda, *Int J Legal Med*, 1997, 110, 1-4.
11. M. Libik, R. Konieczny, B. Pater, I. Slesak and Z. Miszalski, *Plant Cell Rep*, 2005, 23, 834-841.
12. S. M. Somani, K. Husain, C. Whitworth, G. L. Trammell, M. Malafa and L. P. Rybak, *Pharmacol Toxicol*, 2000, 86, 234-241.
13. J. A. Marcusson, B. Carlmark and C. Jarstrand, *Environ Res*, 2000, 83, 123-128.
14. S. Kasperczyk, M. Dobrakowski, A. Kasperczyk, G. Machnik and E. Birkner, *Environ Toxicol Pharmacol*, 2014, 37, 638-647.
15. T. Hackenberg, T. Juul, A. Auzina, S. Gwizdz, A. Malolepszy, K. Van Der Kelen, S. Dam, S. Bressendorff, A. Lorentzen, P. Roepstorff, K. Lehmann Nielsen, J. E. Jorgensen, D. Hofius, F. V. Breusegem, M. Petersen and S. U. Andersen, *Plant Cell*, 2013, 25, 4616-4626.
16. G. S. Ribas, C. R. Vargas and M. Wajner, *Gene*, 2014, 533, 469-476.
17. J. E. Toblli, C. Rivas, G. Cao, J. F. Giani, F. Funk, L. Mizzen and F. P. Dominici, *Chemotherapy research and practice*, 2014, 2014, 570241.
18. H. N. Kirkman, S. Galiano and G. F. Gaetani, *J Biol Chem*, 1987, 262, 660-666.
19. H. N. Kirkman, M. Rolfo, A. M. Ferraris and G. F. Gaetani, *J Biol Chem*, 1999,

274, 13908-13914.
20. G. Cohen and P. Hochstein, *Science*, 1961, 134, 1756-1757.
21. M. D. Scott, T. C. Wagner and D. T. Chiu, *Biochim Biophys Acta*, 1993, 1181, 163-168.
22. G. F. Gaetani, A. M. Ferraris, M. Rolfo, R. Mangerini, S. Arena and H. N. Kirkman, *Blood*, 1996, 87, 1595-1599.
23. K. W. Chang, T. Y. Tsai, K. C. Chen, S. C. Yang, H. J. Huang, T. T. Chang, M. F. Sun, H. Y. Chen, F. J. Tsai and C. Y. Chen, *J Biomol Struct Dyn*, 2011, 29, 243-250.
24. C. Y. Chen, *J Biomol Struct Dyn*, 2009, 27, 271-282.
25. T. Y. Tsai, K. W. Chang and C. Y. Chen, *J Comput Aided Mol Des*, 2011, 25, 525-531.
26. H.-C. Tang and C. Y.-C. Chen, *Evidence-Based Complementary and Alternative Medicine*, 2014, 2014, 13.
27. M.-C. Lin, S.-Y. Tsai, F.-Y. Wang, F.-H. Liu, J.-N. Syu and F.-Y. Tang, *BioMedicine*, 2013, 3, 174-180.
28. H.-J. Huang, H. W. Yu, C.-Y. Chen, C.-H. Hsu, H.-Y. Chen, K.-J. Lee, F.-J. Tsai and C. Y.-C. Chen, *Journal of the Taiwan Institute of Chemical Engineers*, 2010, 41, 623-635.
29. C. Y. Chen, *Curr Top Med Chem*, 2013, 13, 965-988.
30. C.-L. Jao, S.-L. Huang and K.-C. Hsu, *BioMedicine*, 2012, 2, 130-136.
31. S.-C. Hsu, J.-H. Lin, S.-W. Weng, F.-S. Chueh, C.-C. Yu, K.-W. Lu, W. G. Wood and J.-G. Chung, *BioMedicine*, 2013, 3, 120-129.
32. C. Y. C. Chen, *PLoS ONE*, 2011, 6, e15939.
33. C. D. Putnam, A. S. Arvai, Y. Bourne and J. A. Tainer, *Journal of Molecular Biology*, 2000, 296, 295-309.
34. Accelerys, Accelrys Inc. San Diego, CA, USA., 2009.
35. B. Xue, R. L. Dunbrack, R. W. Williams, A. K. Dunker and V. N. Uversky, *Biochim Biophys Acta*, 2010, 1804, 996-1010.
36. M. T. H. Khan, *Curr Drug Metab*, 2010, 11, 285-295.
37. A. Ganesan, *Curr Opin Chem Biol*, 2008, 12, 306-317.
38. T. H. Keller, A. Pichota and Z. Yin, *Curr Opin Chem Biol*, 2006, 10, 357-361.
39. B. R. Brooks, C. L. Brooks, 3rd, A. D. Mackerell, Jr., L. Nilsson, R. J. Petrella, B. Roux, Y. Won, G. Archontis, C. Bartels, S. Boresch, A. Caflisch, L. Caves, Q. Cui, A. R. Dinner, M. Feig, S. Fischer, J. Gao, M. Hodoscek, W. Im, K. Kuczera, T. Lazaridis, J. Ma, V. Ovchinnikov, E. Paci, R. W. Pastor, C. B. Post, J. Z. Pu, M. Schaefer, B. Tidor, R. M. Venable, H. L. Woodcock, X. Wu, W. Yang, D. M. York and M. Karplus, *Journal of Computational Chemistry*, 2009,

30, 1545-1614.
40. R. A. Laskowski and M. B. Swindells, *J Chem Inf Model*, 2011, 51, 2778-2786.
41. S. Pronk, S. Pall, R. Schulz, P. Larsson, P. Bjelkmar, R. Apostolov, M. R. Shirts, J. C. Smith, P. M. Kasson, D. van der Spoel, B. Hess and E. Lindahl, *Bioinformatics*, 2013, 29, 845-854.
42. V. Zoete, M. A. Cuendet, A. Grosdidier and O. Michielin, *Journal of Computational Chemistry*, 2011, 32, 2359-2368.
43. E. Chovancova, A. Pavelka, P. Benes, O. Strnad, J. Brezovsky, B. Kozlikova, A. Gora, V. Sustr, M. Klvana, P. Medek, L. Biedermannova, J. Sochor and J. Damborsky, *PLoS Comput Biol*, 2012, 8, e1002708.
44. T. Yamaguchi, H. Takamura, T. Matoba and J. Terao, *Bioscience, biotechnology, and biochemistry*, 1998, 62, 1201-1204.
45. W. Brand-Williams, M. E. Cuvelier and C. Berset, *LWT - Food Science and Technology*, 1995, 28, 25-30.
46. N. J. Miller, C. Rice-Evans, M. J. Davies, V. Gopinathan and A. Milner, *Clinical science*, 1993, 84, 407-412.
47. J. Zhou, G. Xie and X. Yan, *Encyclopedia of Traditional Chinese Medicines-Molecular Structures, Pharmacological Activities, Natural Sources and Applications: Vol. 6: Indexes*, Springer, 2011.
48. Y. Zhao, C. P. Kao, Y. S. Chang and Y. L. Ho, *Chem Cent J*, 2013, 7, 106.
49. W. I. Tou and C. Y. Chen, *Drug Discov Today*, 2013, DOI: S1359-6446(13)00387-5 [pii]
10.1016/j.drudis.2013.10.020.
50. C. Y. Chen and W. I. Tou, *Drug Discov Today*, 2013, 18, 910-915.
51. W. I. Tou, S. S. Chang, C. C. Lee and C. Y. Chen, *Sci Rep*, 2013, 3, 844.

Table 1. The top ten candidates from docking results, each score were calculated by LigandFit module.

Name	-PMF	DockScore	-PLP1	-PLP2
Cordyceamides A	175.88	82.627	97.18	104.9
Hesperidin	164.51	118.241	109.81	109.24
Grandisin	152.28	80.338	101.63	92.33
THSG	143.74	90.67	65.29	75.64
NADPH*	141.02	79.113	63.06	68.99
Cordyceamides B	138.05	84.51	92.19	99.34
(-)-Trifolirhizin	127.79	86.353	92.02	89.04
Coniferylferulate	125.16	79.97	93.47	94.53
Angeliferulate	123.07	90.597	92.2	90.81
Casimiroedine	118.46	91.049	101.7	101.07
Ningposides A	111.36	94.151	105.45	105.26

*Control

Table 2. The DPPH radical scavenging capacity of Hesperidin and THGS

Name	[a] Conc. (μg/mL)	[a] Conc. (μM)	[b] Abs.	EC_{50} (μg/mL)
Hesperidin	240.00	393.08	0.79	＞240
THGS	148.00	364.19	0.33	105.80 ± 0.974
	74.00	182.10	0.53	
[c] BHT	92.50	419.78	0.25	47.73 ± 0.601
	46.25	209.90	0.45	

Each value represents the mean ± SD (n = 3).

[a] Concentration

[b] Absorbance

[c] Positive control

Table 3. The antioxidant capacity of TEAC assay

Name	TEAC (μmol Trolox/mg)
Hesperidin	146.31 ± 11.92
THGS	626.31 ±30.73
[a] BHT	449.44 ±17.98

Each value represents the mean ± SD (n = 3).

[a] Positive control

Figure Legend

Figure 1. The chemical scaffold of the TCM candidates and control: (a) Hesperidin (b) THSG (c) NADPH.

Figure 2. 2D diagram of docking poses of complex with (a) Hesperidin (b) THSG (c) NADPH descripted by DS 2.5 program. The pi interaction is represented by orange line.

Figure 3. Protein-ligand interaction diagrams of complex with (a) Hesperidin (b) THSG (c) NADPH descripted by LigPlot plus program.

Figure 4. The disorder prediction of sequence of catalase, a value of disorder description below 0.5 indicates order residues. The key binding residues are represented by blue line.

Figure 5. Trajectory analysis of (a) Protein and (b) ligand by RMSD analysis

Figure 6. Trajectory analysis of (a) protein gyrate and (b) mean square deviation (MSD).

Figure 7. Total energy calculation of complex with (A) Hesperidin (B) THSG (C) NADPH during simulation time of 5ns.

Figure 8. RMSF analysis of complex with (a) Hesperidin (b) THSG (c) NADPH during simulation time of 5ns.

Figure 9. Cluster analysis of complex with (a) Hesperidin (b) THSG (c) NADPH during simulation time of 5ns.

Figure 10. The distance variation between the centers of mass of catalase and docked ligand: (a) Hesperidin (b) THSG (c) NADPH during simulation time of 5ns.

Figure 11. The distance variation between acceptor and donor atoms of residue and docked ligand: (a) Hesperidin (b) THSG (c) NADPH during simulation time of 5ns.

Figure 12. The secondary structure analysis for catalase with the docked ligand: (a) Hesperidin (b) THSG (c) NADPH over all simulation time.

Figure 13. Matrices of smallest distance between each residue on catalase with the docked ligand: (a) Hesperidin (b) THSG (c) NADPH over all simulation time.

Figure 14. Number of frames of first two eigenvectors (PC1 and PC2) for catalase contains the docked ligand: (a) Hesperidin (b) THSG (c) NADPH.

Figure 15. Projection of first two eigenvectors (PC1 and PC2) of each complex for principle component analysis in phase space: (a) Hesperidin (b) THSG (c) NADPH

Figure 16. Ligand tunnel prediction of catalase contains the docked ligand: (a) Hesperidin (b) THSG (c) NADPH.

Figure 17. The calibration curve ($R^2 = 0.9989$) of trolox.

1

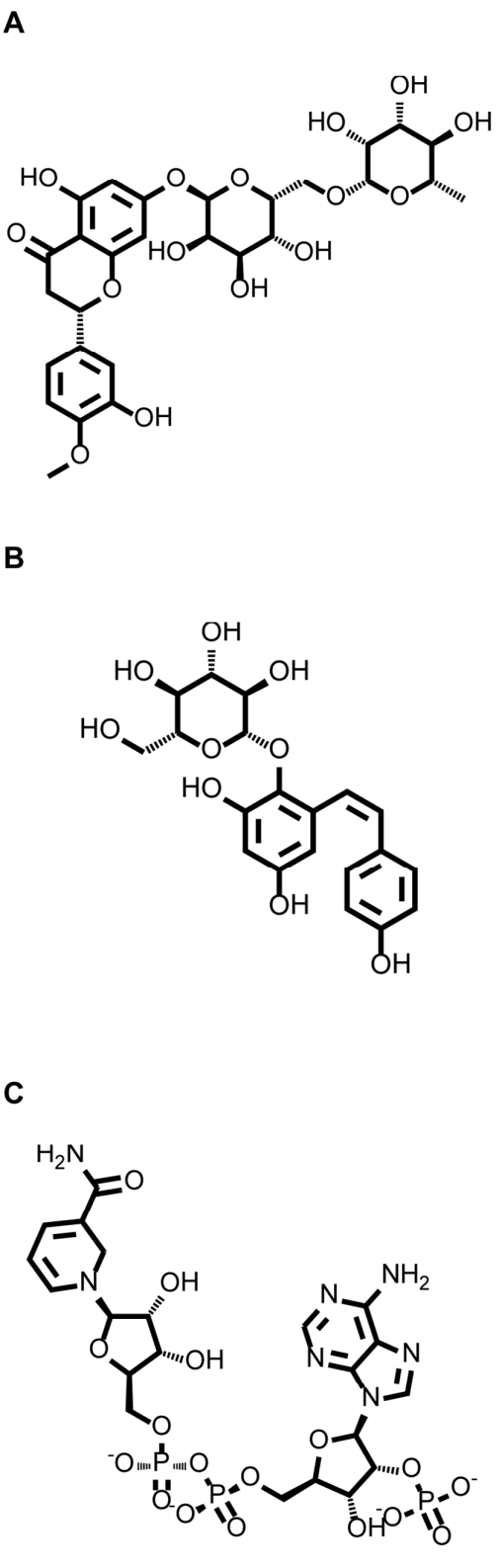

2

3 Figure 1.

4

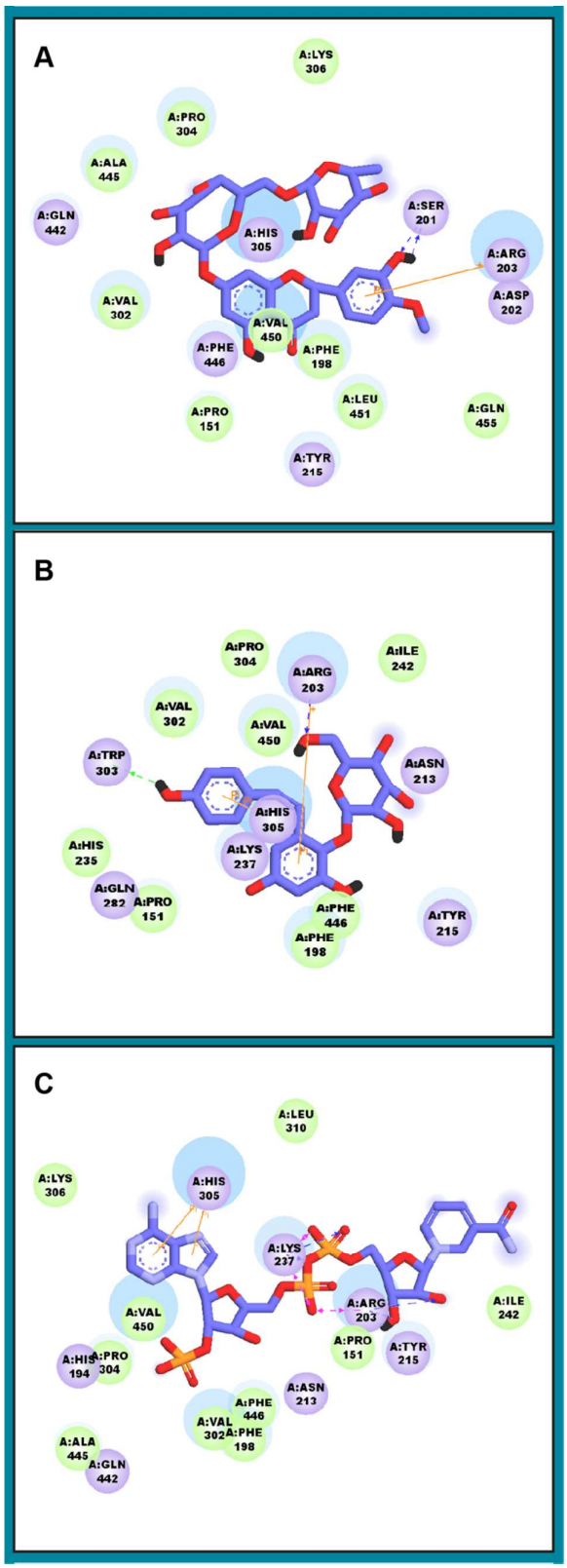

Figure 2.

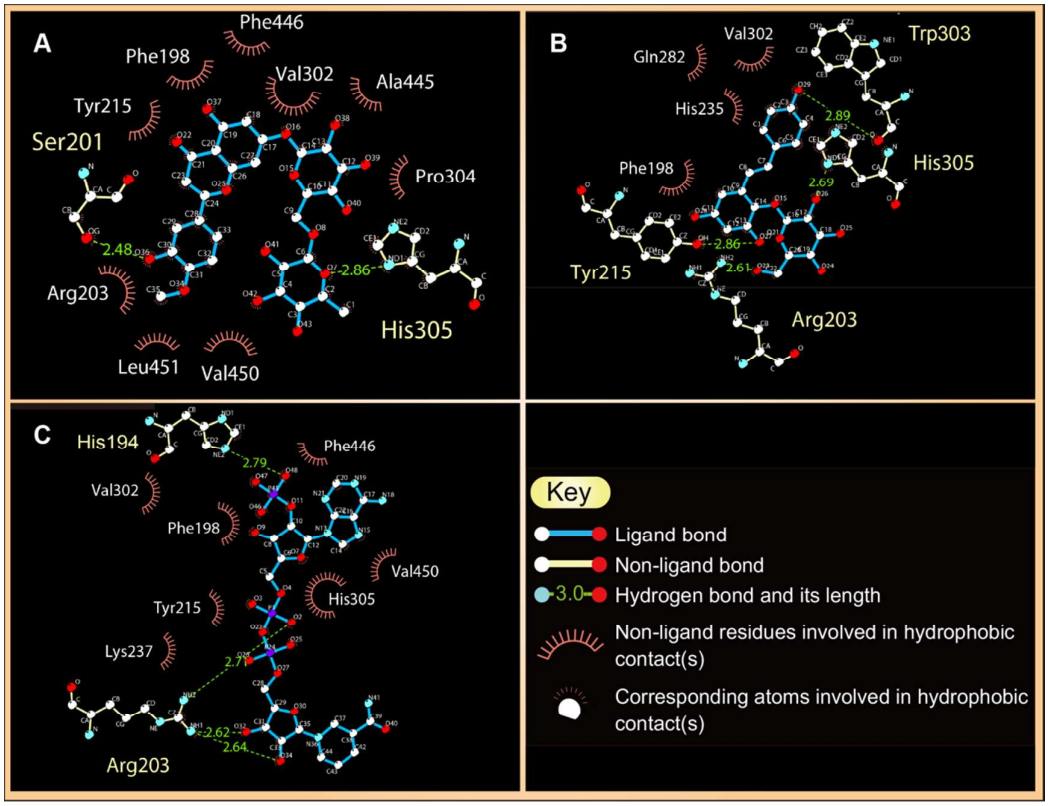

Figure 3.

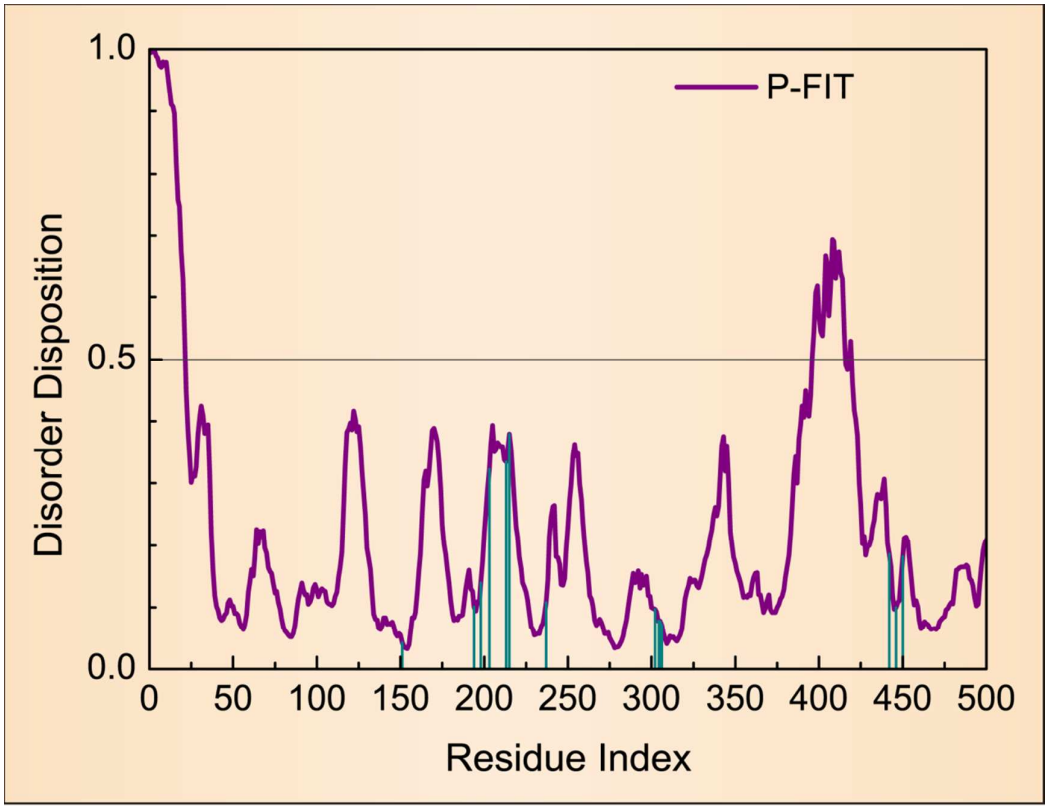

Figure 4.

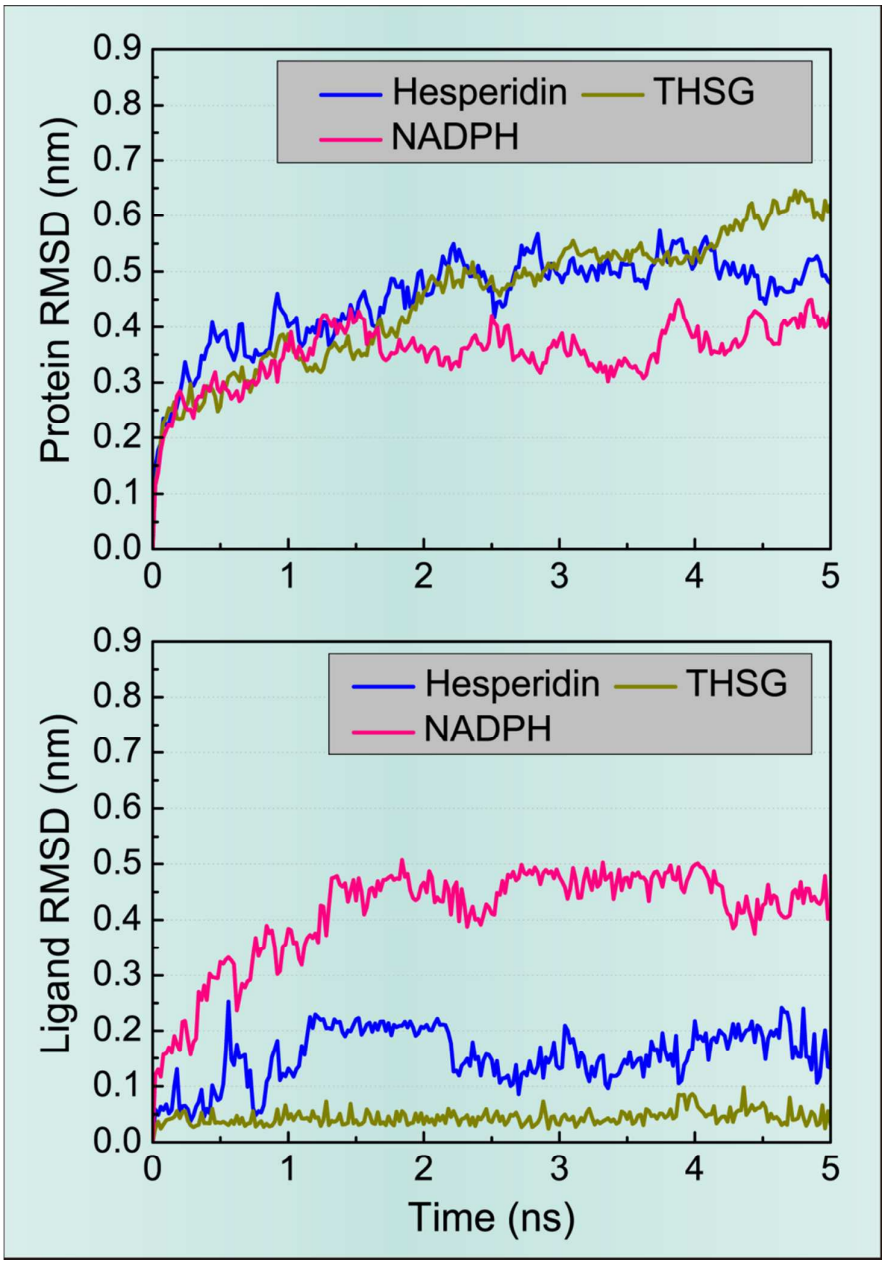

Figure 5.

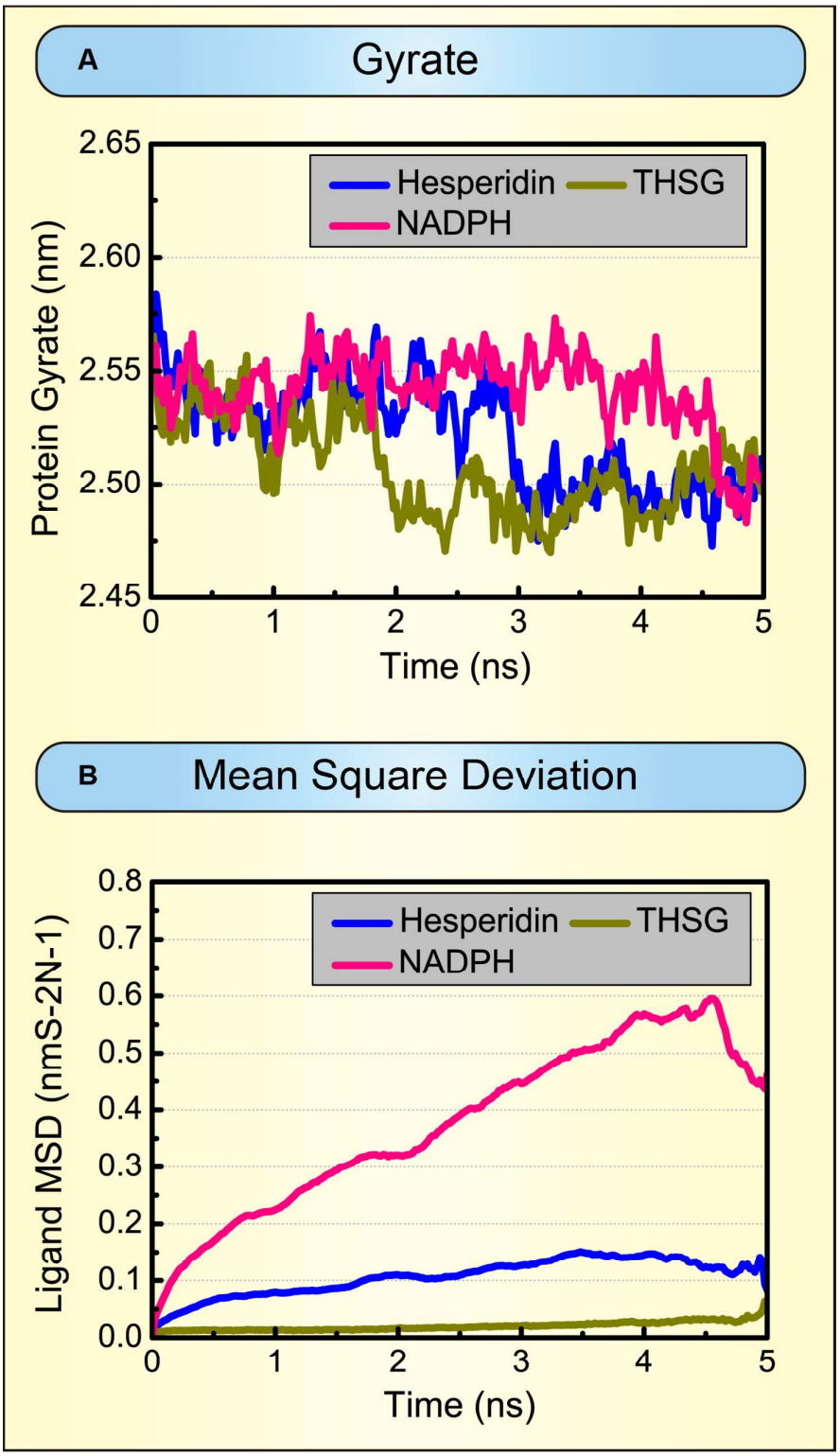

Figure 6.

1

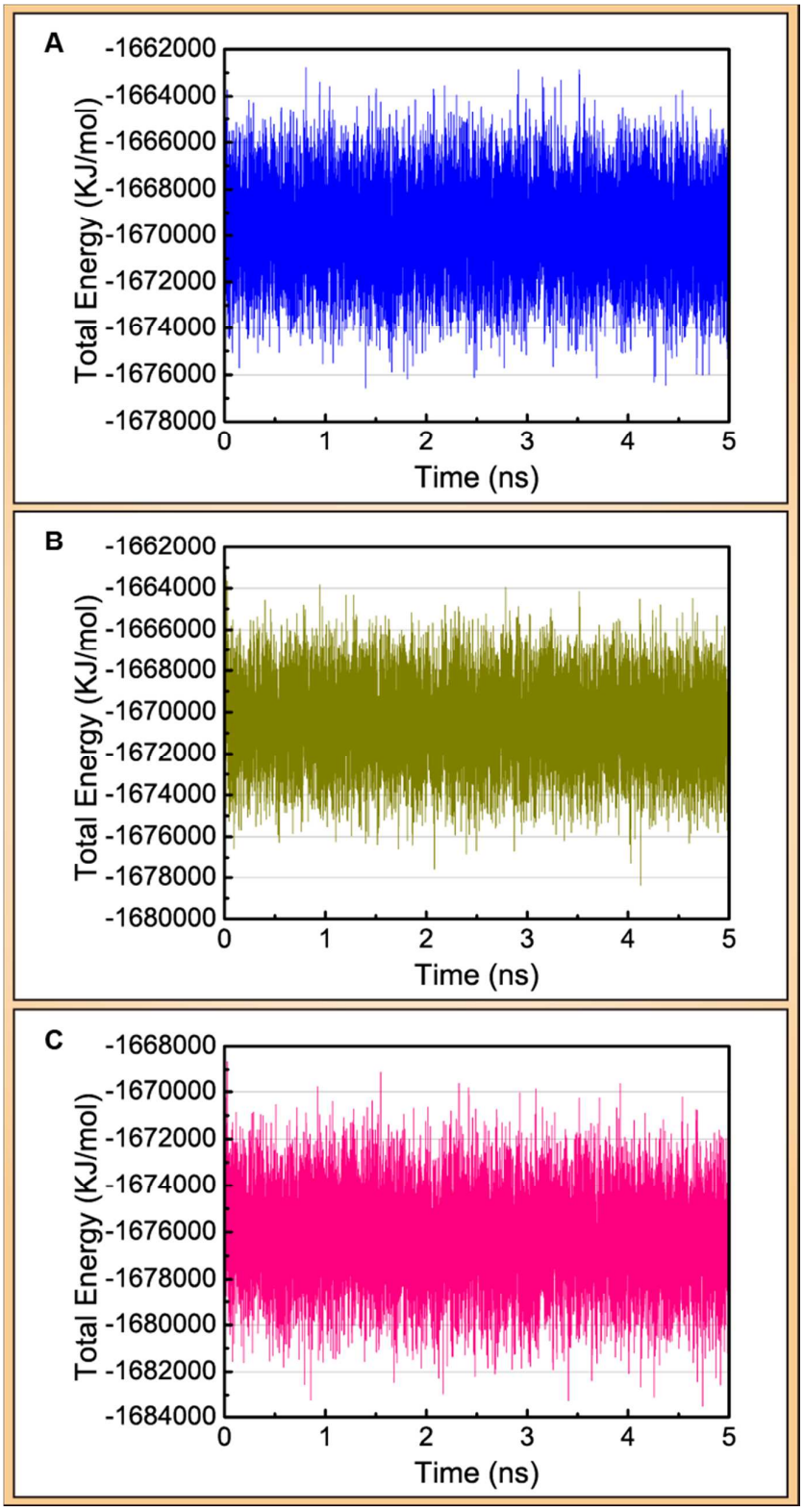

2

3 Figure 7.

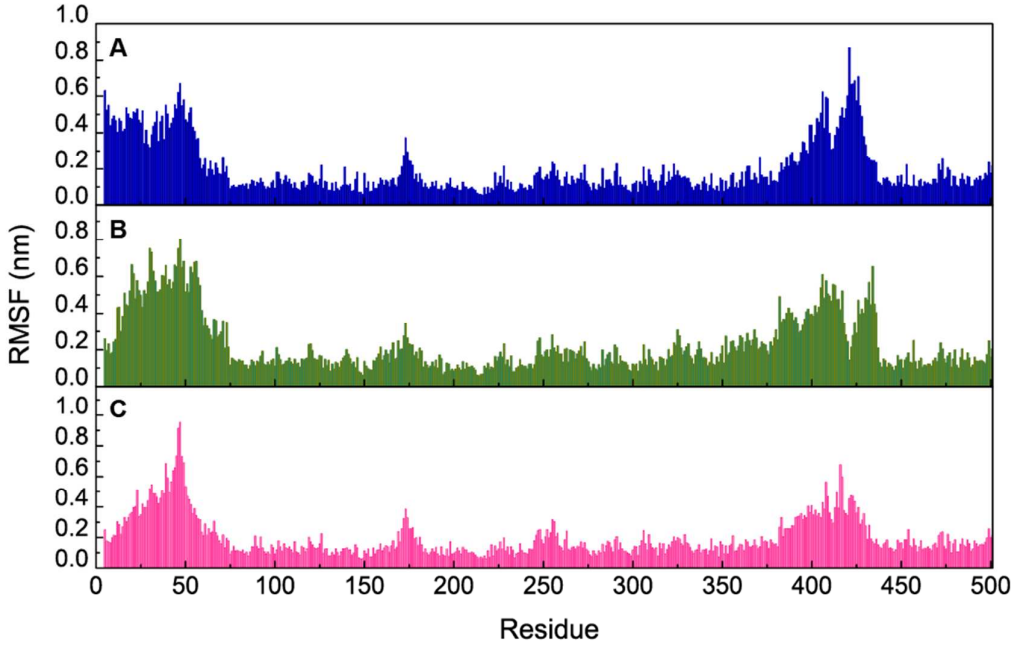

Figure 8.

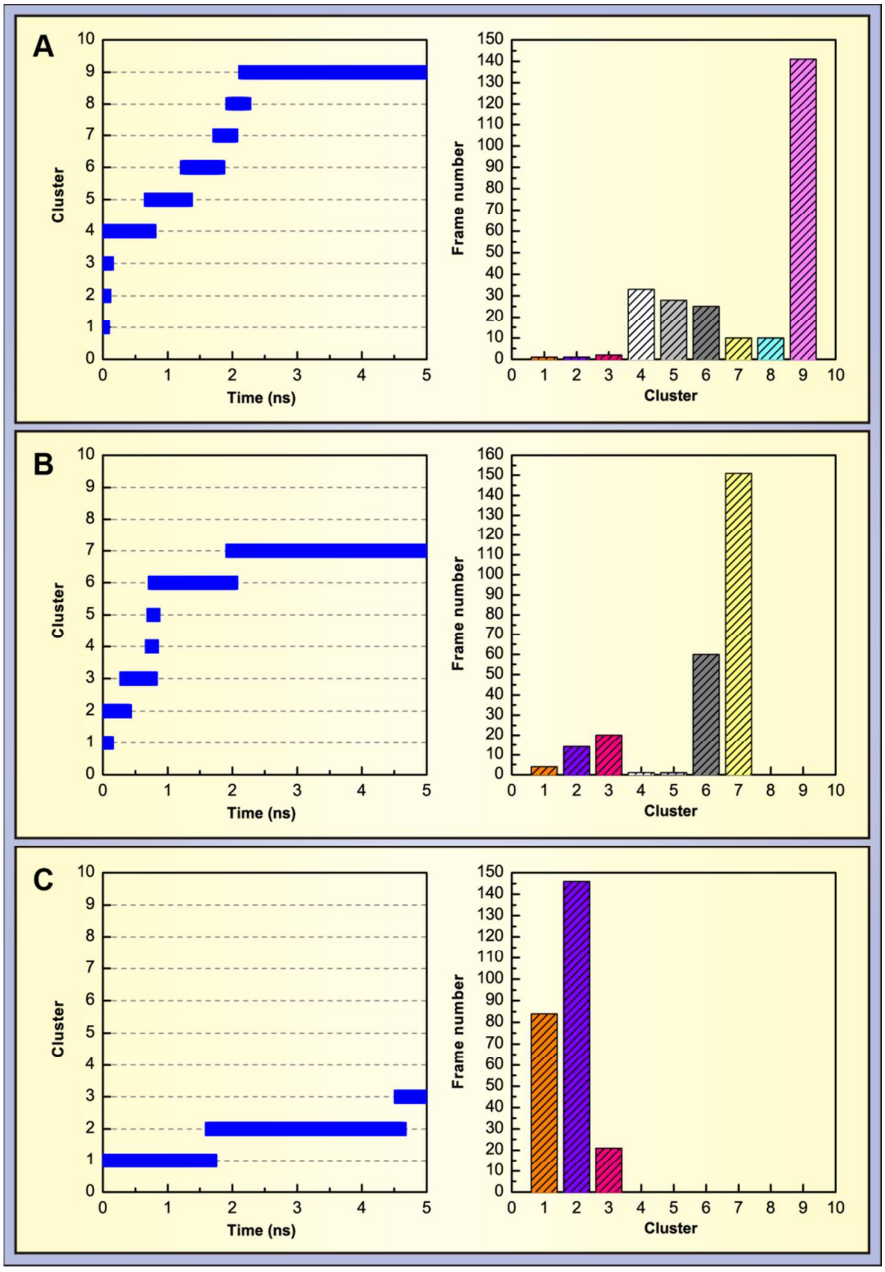

Figure 9.

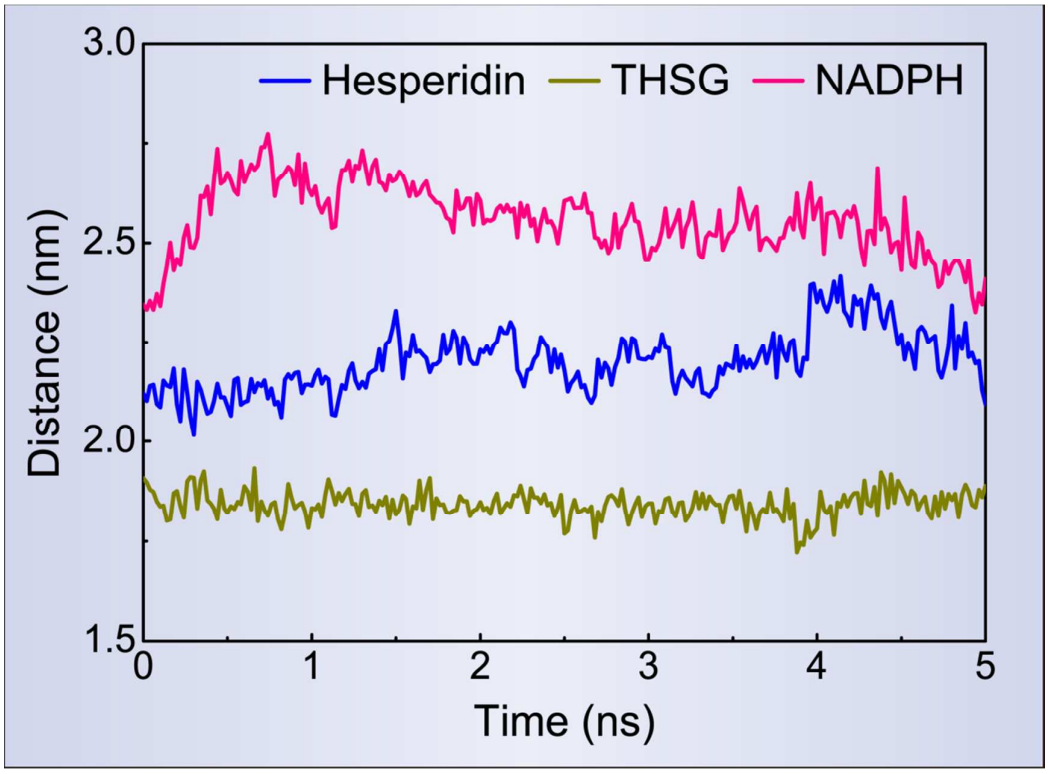

Figure 10.

1

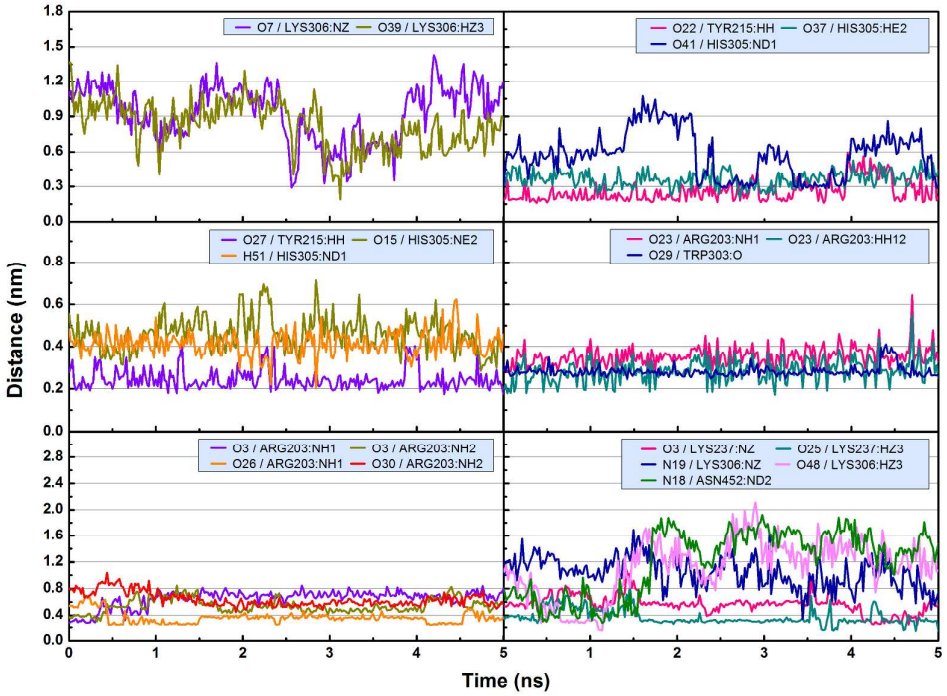

2

3 Figure 11.

4

5

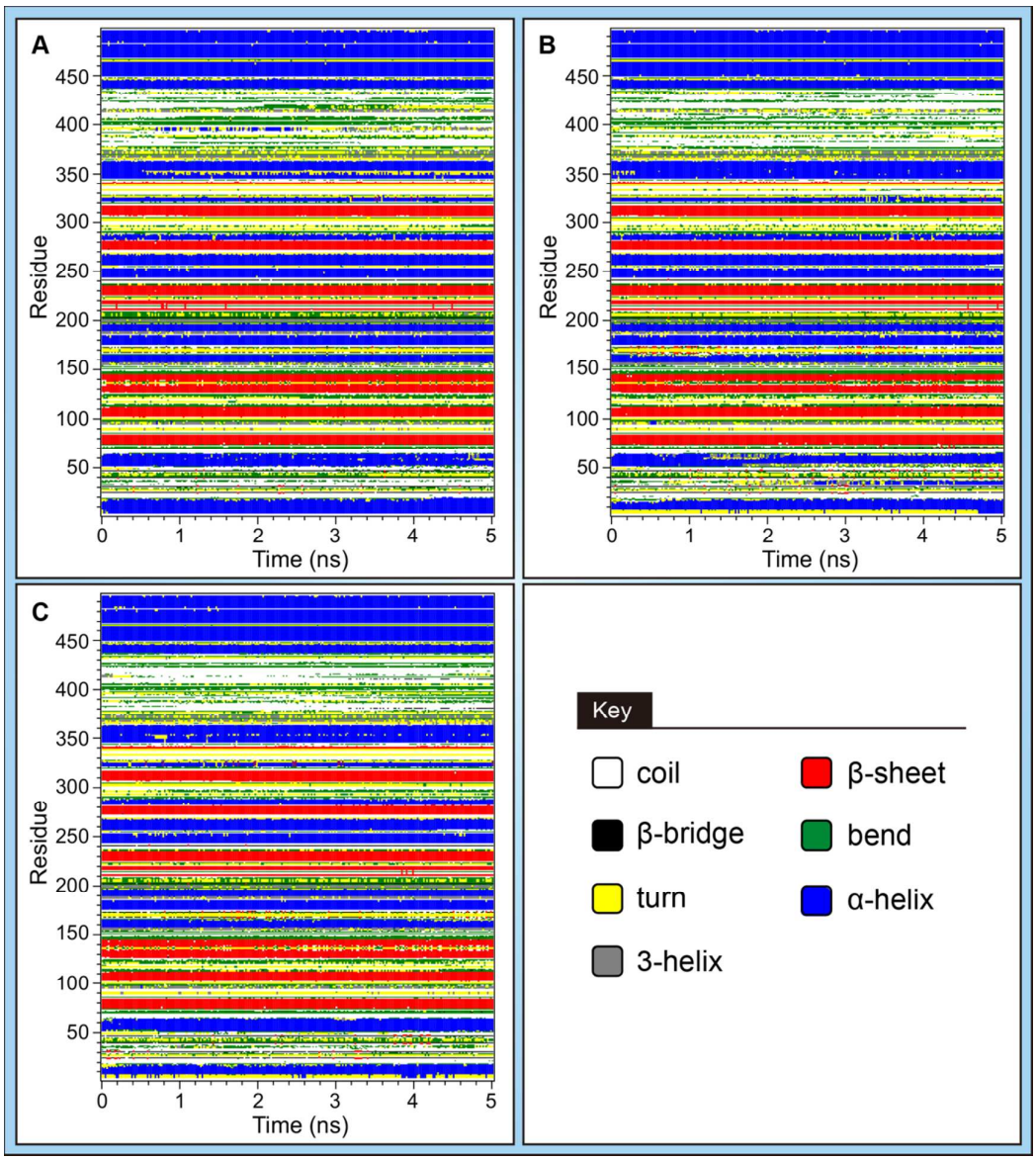

Figure 12.

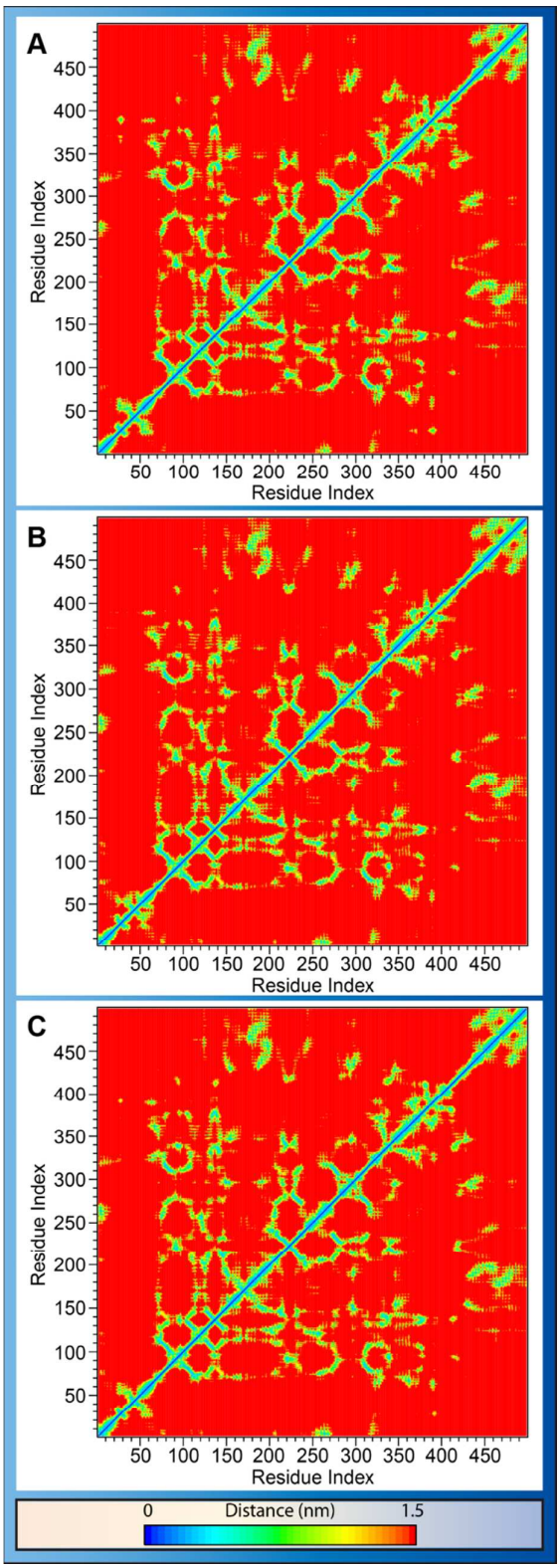

Figure 13.

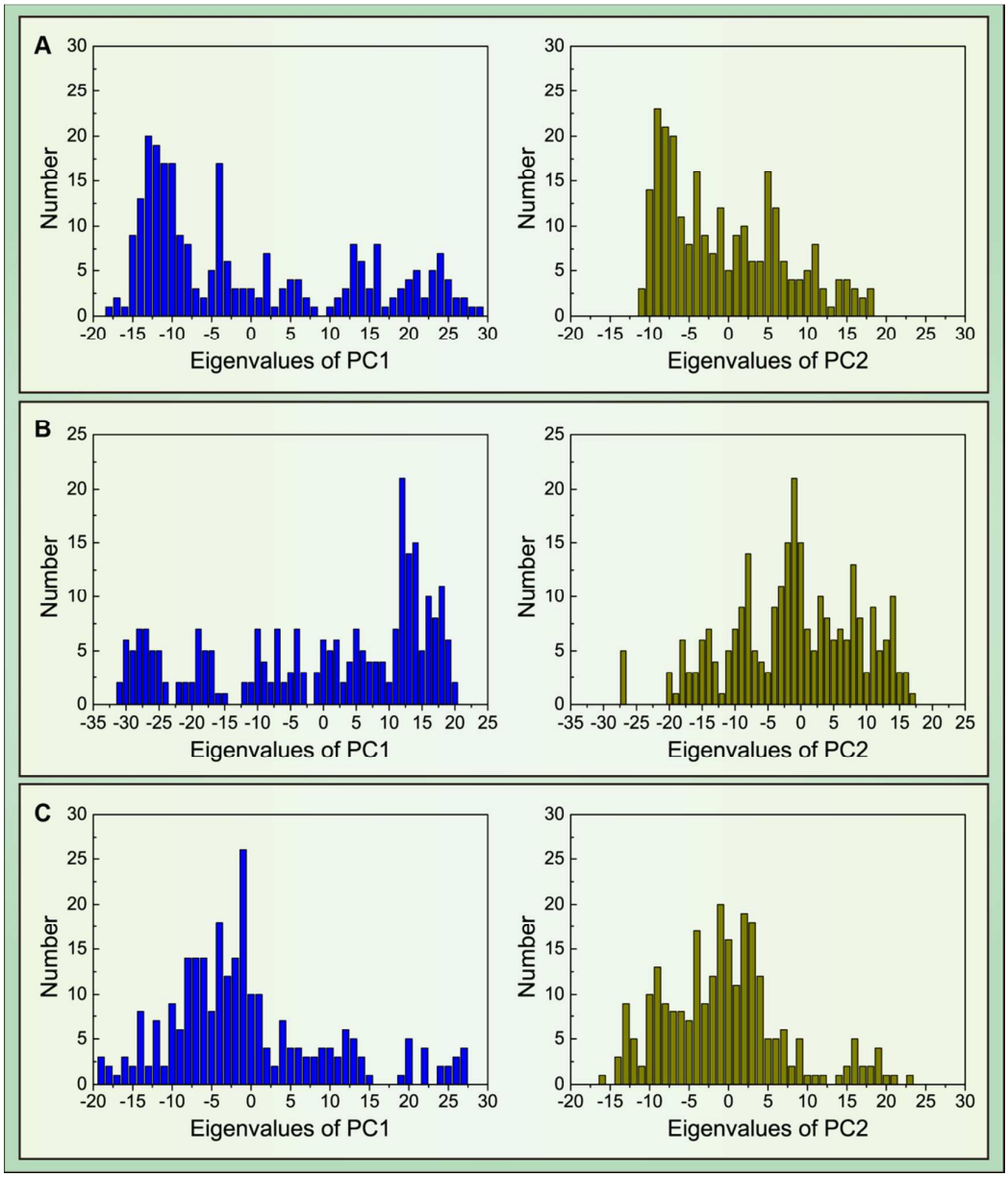

Figure 14.

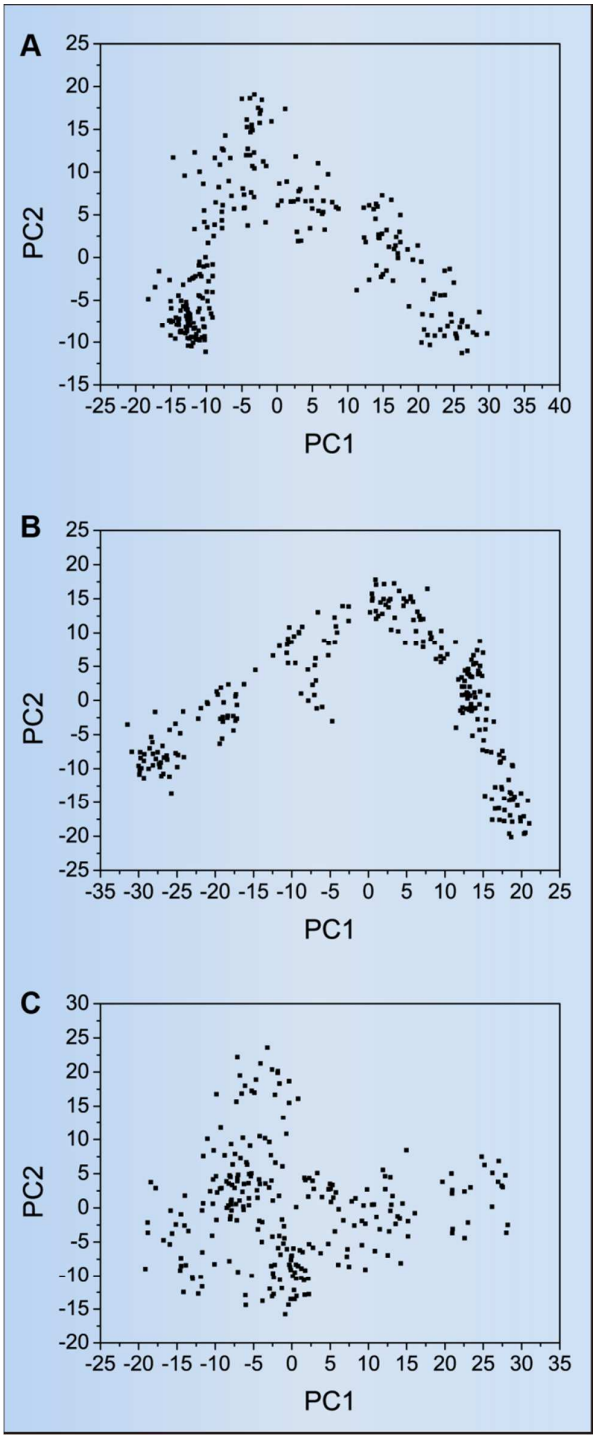

Figure 15.

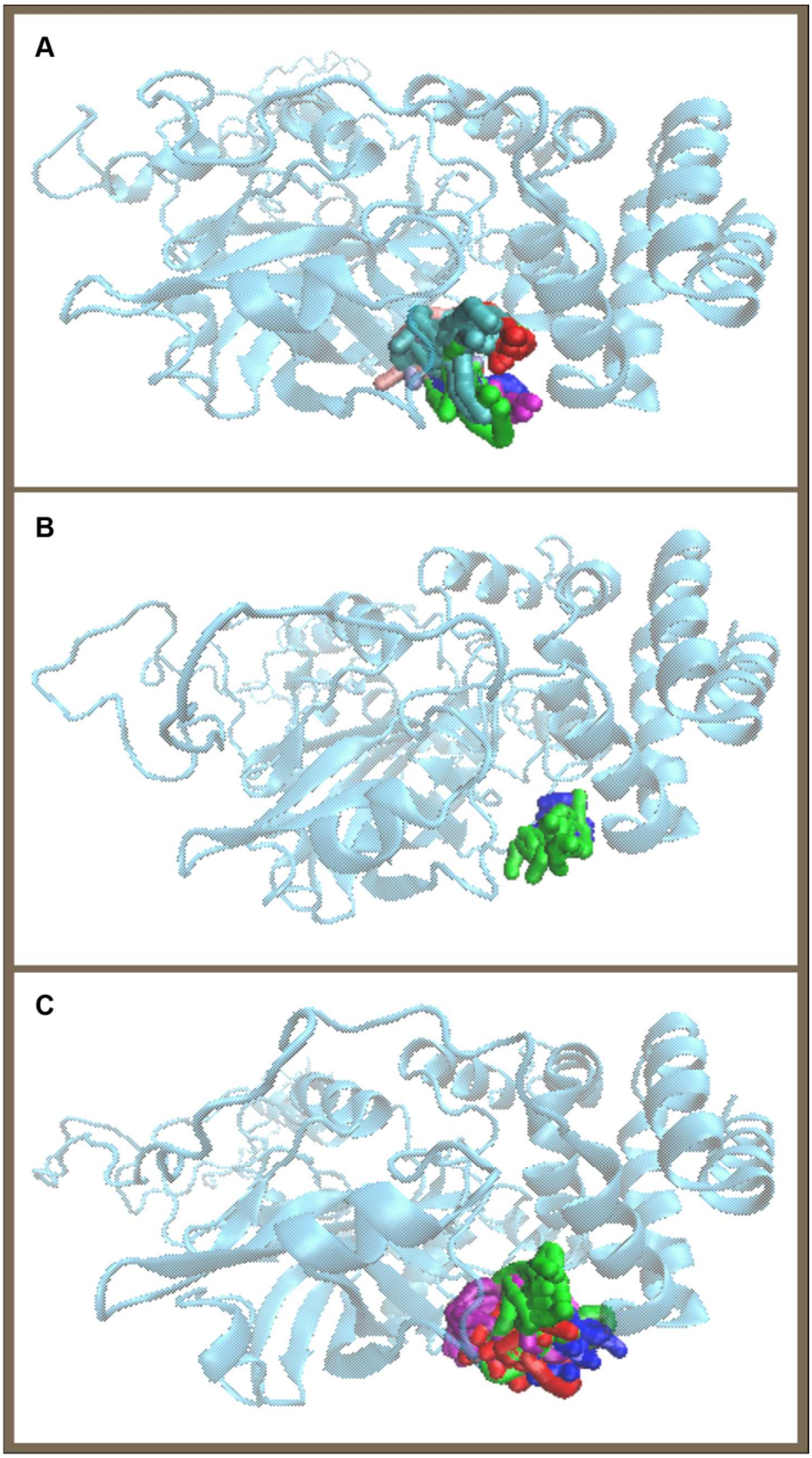

Figure 16.

1

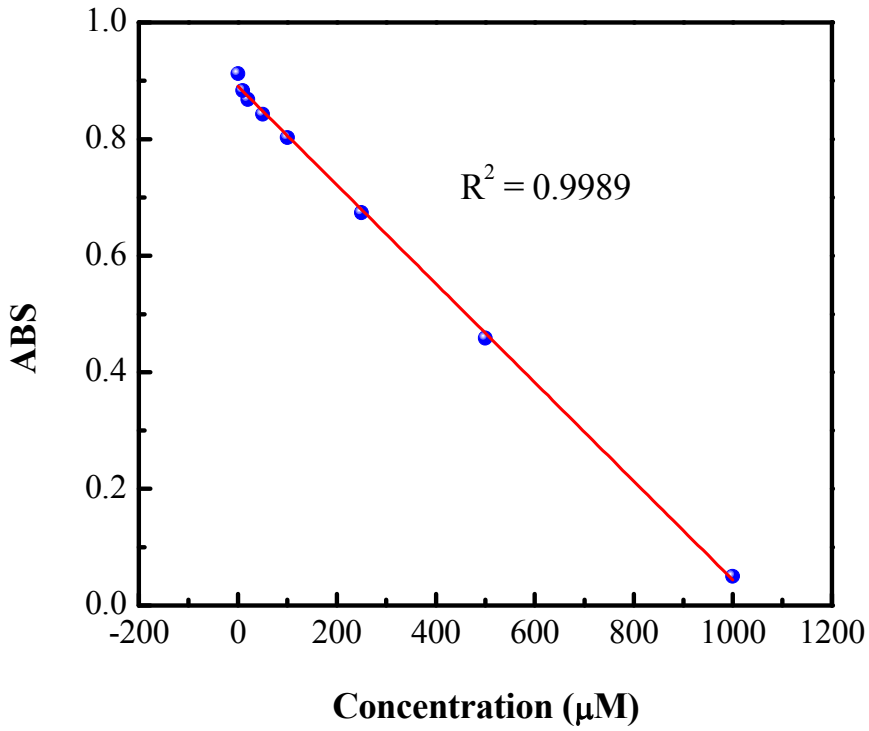

2

3 Figure 17.